National Conference with International Participation

ENGINEERING MECHANICS 2008

Svratka, Czech Republic, May 12 – 15, 2008

PHASE-LOCAL CONTACT OF TEETH OF SCREW COMPRESSOR

V. Machulda[*], J. Švígler [**]

.

Summary: *This contribution is devoted to screw compressors with injection, where tooth surfaces provide kinematic and force coupling between rotors. In theoretical case axes of both rotors are parallel. Under influence of operating loading, which is composed of force field, temperature field and dynamic activities, the parallel arrangement of rotor axes changes into skew position and a curvilinear correct contact between tooth surfaces of rotors changes into the incorrect contact at point. Aim of this contribution is determination of the position of the contact point between two conjugated screw surfaces by skew arrangement of rotors axes in time period.*

1. Introduction

The most important part of screw machines, which are represented by screw compressors and screw motors, are rotors with screw curved teeth. This contribution is devoted to screw compressors with injection, Fig. 1, where tooth surfaces provide kinematic and force joint between rotors.

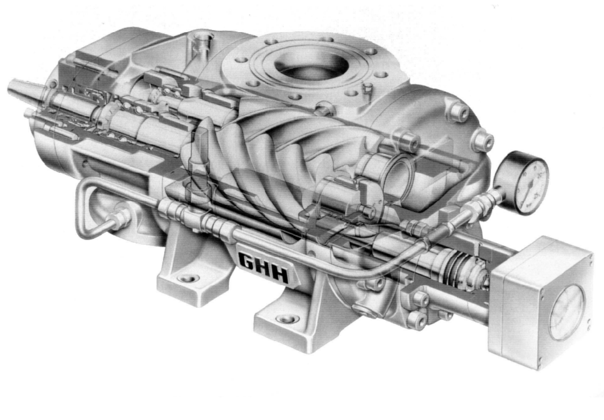

Fig. 1: Screw compressor with injection

In theoretical case axes of both rotors are parallel and relative movement is determined by the rolling of both rotors. In this case it is possible kinematic problems and some solution of

[*] Ing. Vladimír Machulda: Department of Mechanics, University of West Bohemia in Pilsen, Univerzitní 22, 306 14 Plzeň; tel.: +420 377 632 382, fax: +420 377 632 302; e-mail: machulda@kme.zcu.cz

[**] Doc. Ing. Jaromír Švígler, CSc.: Department of Mechanics, University of West Bohemia in Pilsen, Univerzitní 22, 306 14 Plzeň; tel.: +420 377 632 324, fax: +420 377 632 302; e-mail: svigler@kme.zcu.cz

static and dynamic problems to think as planar problem in cross sections of rotors at the given time. Under the influence of the force field, temperature field and dynamic activities the parallel arrangement of rotor axes changes into skew position and correct contact between tooth of rotors, which is curvilinear in theoretical case, changes into incorrect contact at point. Aim of this contribution is determination of position of contact point by skew arrangement of rotors axes in time period.

Numerical solution was made for next basic geometric parameters of the screw machine: axes distance a_w = 85 mm, gear ratio i_{32} = 1.2, where 3 is male rotor and 2 is female rotor, helix angle on the rolling cylinder of both rotors γ = 45, length of tooth part of both rotors l = 193.8 mm, radius of pitch circle of male rotor r_{w3} = 46.3635 mm, radius of pitch circle of female rotor r_{w2} = 38.6365 mm.

2. Modelling of tooth surfaces of rotors

Profile of one tooth of female rotor is created by curves k_i, where i = 1, 3, 5, 7, 9, 11. Curves k_1, k_3, k_7, k_{11} are created with circle arcs, curve k_5 is trochoid curve and curve k_9 is created with the line segment.

Profile of tooth of conjugated male rotor is created by set of curves k_j, j = 2, 4, 8, 10, 12, which are created as envelopes of curves k_i of female rotor curves without trochoid k_5. Curve k_6 degenerates into a point. Exact description of creation of conjugated teeth is described in Švígler&Albl (1995). Profiles of both rotors are demonstrated in Fig. 2.

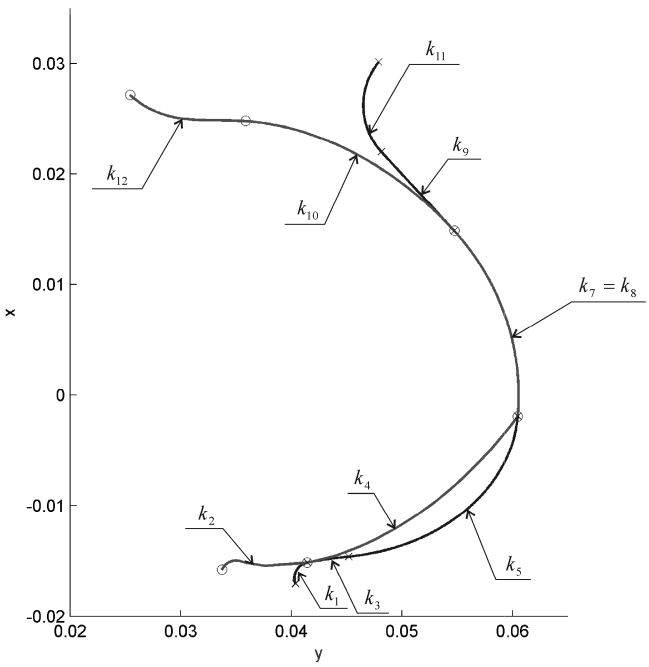

Fig. 2: Profiles of meshing teeth

Tooth surfaces along the length of rotors are created by screw motion of tooth profiles, angle ψ_i and axial displacement z_i, $i = 2, 3,$ along axes o_i of rotors. This screw motion is determined by equation

$$\mathbf{r}_i(\psi_i, u_j) = \begin{bmatrix} \cos\psi_i & -\sin\psi_i & 0 & 0 \\ \sin\psi_i & \cos\psi_i & 0 & 0 \\ 0 & 0 & 1 & z_i \\ 0 & 0 & 0 & 1 \end{bmatrix} \begin{bmatrix} \mathbf{r}_i(u_j) \\ 1 \end{bmatrix}, \tag{1}$$

where u_j is a parameter of profile curves, $\mathbf{r}_i(\psi_i, u_j)$ is a position vector of point of surface and $z_i = r_{wi}\psi_i \tan\gamma, i = 2, 3,$ is the axial displacement along the rotor axis. For $\psi_i = 0$ the position vector $\mathbf{r}_i(u_j)$ determines the position of this point in frontal cross-section.

3. Correct contact

In ideal case the contact between conjugated tooth profiles is curvilinear. In each point of curve of contact, the characteristic curve, the condition (2) has to be satisfied. This condition expresses perpendicularity between the normal vector $\mathbf{n}_L$ and the vector of relative velocity $\mathbf{v}_{L32}$ in the contact point L.

$$\mathbf{n}_L \cdot \mathbf{v}_{L32} = 0. \tag{2}$$

In the case that generating profile is created by arc of circle the condition (2) can be rewritten into form

$$f(\chi, \psi_{3L}, \varphi_3) = (i_{32} + 1) r_S \sin(\chi - \Phi) + a_w \sin(\varphi_3 + \psi_{3L} + \chi) = 0, \tag{3}$$

where r_S and Φ determine position of circle center and χ determines position of point on arc. The contact point condition in the case of line segment is expressed with the equation

$$f(\chi, \psi_{3L}, \varphi_3) = (i_{32} + 1)(x_A \cos\varepsilon + y_A \sin\varepsilon + \chi) - a_w \sin(\varphi_3 + \psi_{3L} + \varepsilon) = 0. \tag{4}$$

With using the equation (2) the characteristic curve can be determined at instantaneous time. In Fig. 3 the projection of characteristic curve to plane xz is shown and the projection of this same to the frontal plane is demonstrated in Fig. 4. A dash part of the curve in Fig. 3 determines a section of this curve which lies on sealing side of teeth.

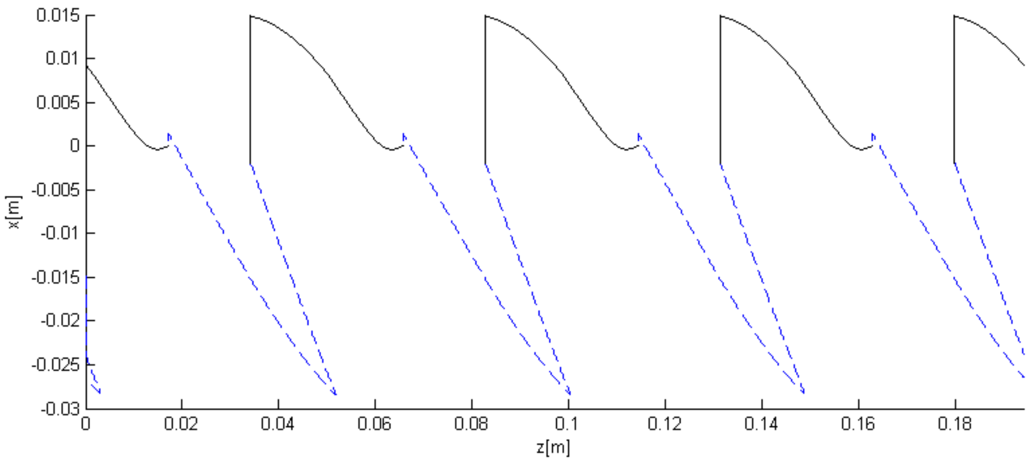

Fig. 3: Projection of characteristic curve to plane xz

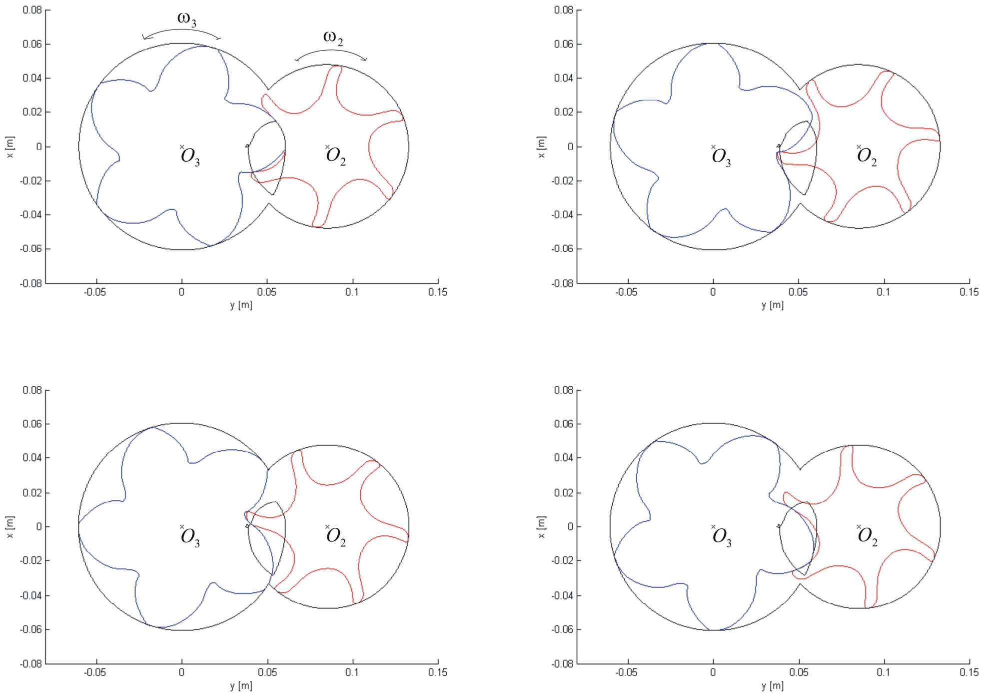

Fig. 3: Projection of characteristic curve to cross-section

4. Incorrect contact

4.1. Heat and force deformation

Deformation of the housing and bearing of screw compressor is caused by heat and force loading. Housing and bearing deformation leads to incorrect contact of conjugated surfaces of teeth, Stosic et al. (2003). We consider heat and force deformation of screw compressor housing constant. The numerical solution of force housing deformation was made using the software package software ANSYS. Vectors of deformations at center of bearings are presented in Tab.1, see Švígler et al. (2007). The numerical solution of screw compressor heat housing deformation was made using the software package software MSC.Mark on the ground of experimental determined temperature field. Vectors of deformations at center of bearings are shown in Tab.2, Kleisner (2006). These vectors are identified as $\mathbf{d}_{X_{ia}}$, where, Fig.5, $X = A, B$, $i = 2, 3$, $a = f, t, b$. A means the frontal side bearing, B means the back side bearing, 2 or 3 means female or male rotor and *f*, *t* means force and temperature deformation of housing and *b* is bearing deformation respectively.

Tab. 1: Force housing deformation

$\mathbf{d}_{A_{3f}}$ $[\mu m]$	$\mathbf{d}_{A_{2f}}$ $[\mu m]$	$\mathbf{d}_{B_{3f}}$ $[\mu m]$	$\mathbf{d}_{B_{2f}}$ $[\mu m]$
-0.212 -0.221 0.720	1.226 -0.071 -1.585	0.020 -0.203 -0.659	1.711 -0.116 -1.595

Tab. 2: Heat housing deformation

$\mathbf{d}_{A_{3t}}\,[\mu m]$	$\mathbf{d}_{A_{2t}}\,[\mu m]$	$\mathbf{d}_{B_{3t}}\,[\mu m]$	$\mathbf{d}_{B_{2t}}\,[\mu m]$
39.241	58.407	18.852	35.380
-45.776	-52.355	26.710	23.807
0	0	0	0

In the case of bearing deformation it is necessary to determine forces in bearings as it is shown in Švígler et al. (2007). We determine action force $\mathbf{F}_{Xi}$, where indexes X and i have the same meaning as in the case of vectors of deformation, for four time levels. Vectors of action forces in the first time level are introduced in Tab. 3.

Tab. 3: Action force in bearings

$\mathbf{F}_{A_3}\,[N]$	$\mathbf{F}_{A_2}\,[N]$	$\mathbf{F}_{B_3}\,[N]$	$\mathbf{F}_{B_2}\,[N]$
670.96	821.17	1377.55	1466.09
-901.69	812.40	-1484.59	1595.42
0	0	-1251.39	-313.54

With using of relations (5) and (6), Fröhlich (1980), the deformation of bearing center can be calculated. F_i, i = r, a, is value of force in radial and axial direction, Q_i, $i = r, a$, is loading of roller element, δ_i, $i = r, a$, is elastic displacement, l_a is effective length of element, z is number of elements and α is contact angle of elements.

$$Q_r \doteq \frac{5F_r}{z\cos\alpha},\ \delta_r \doteq 7.68\cdot 10^{-5}\,\frac{Q_r^{\,0.9}}{l_a^{\,0.8}\cos\alpha}, \tag{5}$$

$$Q_a \doteq \frac{F_a}{z\sin\alpha},\ \delta_a \doteq 7.68\cdot 10^{-5}\,\frac{Q_a^{\,0.9}}{l_a^{\,0.8}\sin\alpha}. \tag{6}$$

Vectors of bearing deformations in four time levels are shown in Tab. 4 and dependence of components of these vectors on rotation of the male rotor is shown in Fig. 5 - Fig. 8, where on the left side is bearing of male rotor and on the right side is bearing of female rotor.

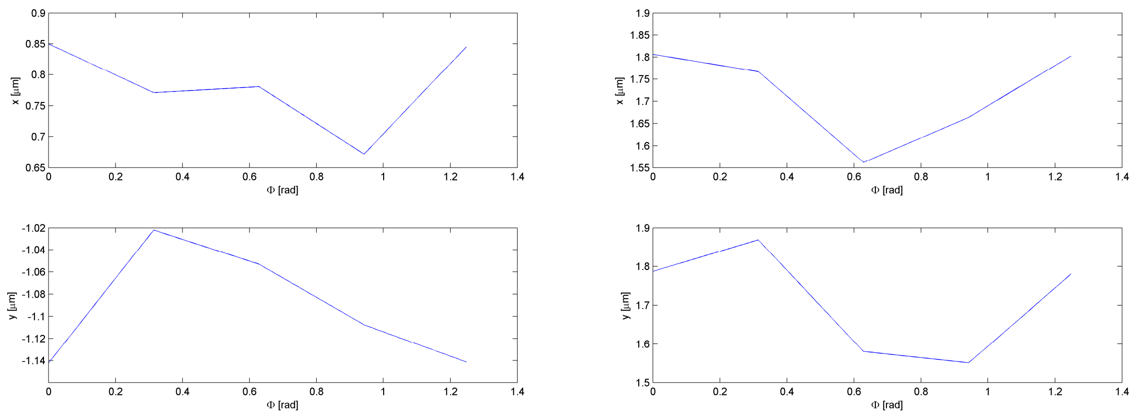

Fig. 5: Components of deformation of bearing centers on the frontal side

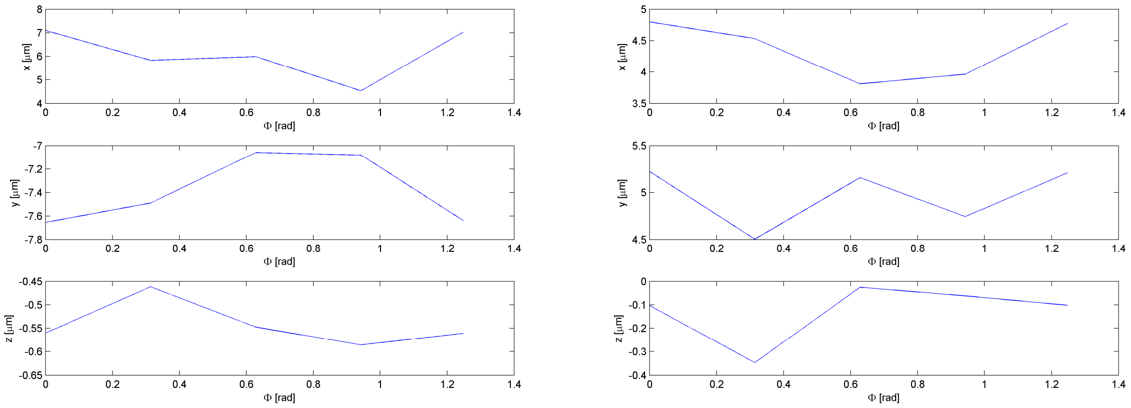

Fig. 6: Components of deformation of bearing centers on the back side

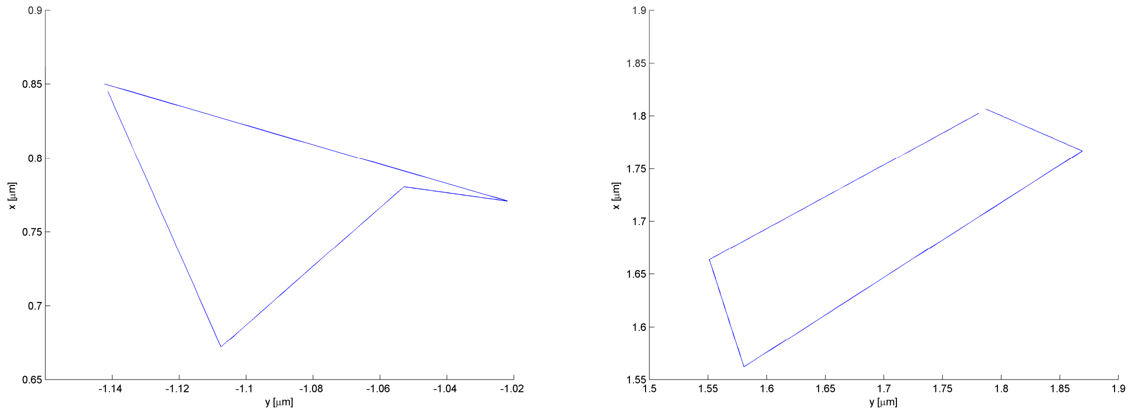

Fig. 7: Deformation of bearing centers on the frontal side

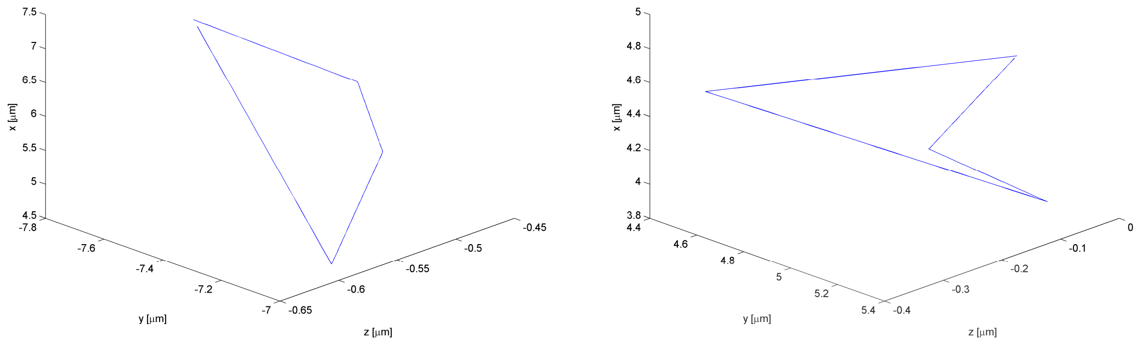

Fig. 8: Deformation of bearing centers on the back side

Tab. 4: Bearing deformations in time levels

Time level	$\mathbf{d}_{A_{3b}}\ [\mu m]$	$\mathbf{d}_{A_{2b}}\ [\mu m]$	$\mathbf{d}_{B_{3b}}\ [\mu m]$	$\mathbf{d}_{B_{2b}}\ [\mu m]$
	0.840	1.799	7.1026	4.7986
1	-1.140	1.774	-7.6545	5.2219
	0	0	-0.5602	-0.103
	0.7753	1.7693	5.8322	4.533
2	-1.0287	1.8645	-7.4895	4.5037
	0	0	-0.4614	-0.3469
	0.7801	1.5736	5.9895	3.8098
3	-1.0512	1.5965	-7.0591	5.1571
	0	0	-0.5475	-0.0253
	0.6782	1.6580	4.5328	3.964
4	-1.1045	1.5527	-7.0810	4.7442
	0	0	-0.5857	-0.0619

4.2. Determination of contact point

Primarily we determine total deformation of bearing centers accordance with equation (9). Deformation of axes position of both rotors is simulated by translation and subsequently by turning of female rotor axis, Fig. 9. Position of point $O_2{}^{\Delta}$ and unit vector of axis $o_2{}^{\Delta}$ are determined by using of position vectors of bearing centers in the coordinate system $R \in (\mathbf{i}, \mathbf{j}, \mathbf{k})$ of basic space. These position vectors are defined by equation (10), where $\mathbf{r}_{Xi}$ are position vectors of bearing centers in ideal case, Tab. 5.

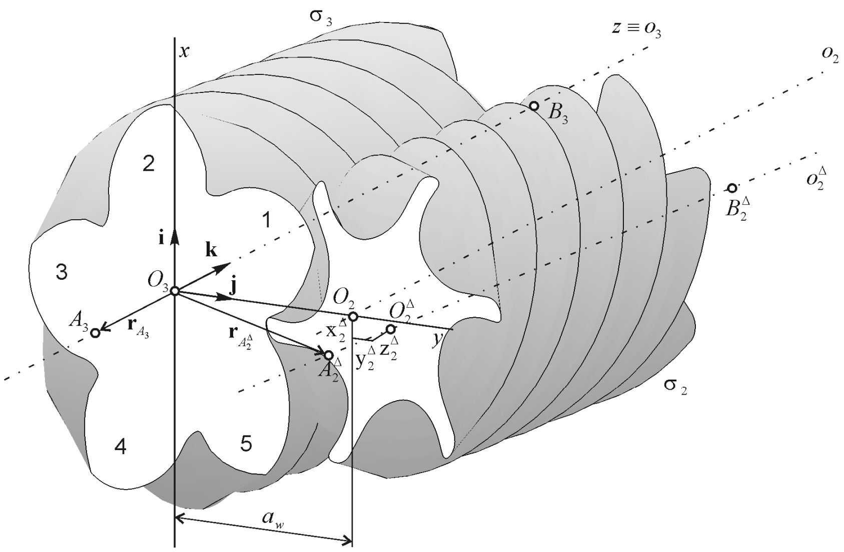

Fig. 9: Deformed rotors position and its coordinate system

$$\mathbf{d}_{X_i} = \mathbf{d}_{X_{if}} + \mathbf{d}_{X_{it}} + \mathbf{d}_{X_{ib}}, \tag{9}$$

$$\mathbf{r}_{X_i^\Delta} = \mathbf{r}_{X_f} + \mathbf{d}_{X_t}. \tag{10}$$

Tab. 5: Position of bearing centers in ideal case

$\mathbf{r}_{A_3}\,[mm]$	$\mathbf{r}_{A_2}\,[mm]$	$\mathbf{r}_{B_3}\,[mm]$	$\mathbf{r}_{B_2}\,[mm]$
0	0	0	0
0	85	0	85
-30	235.8	-22	247.8

For determination of the contact point of conjugated tooth surfaces, which are at incorrect position, the numerical solution was used. This solution is founded on discrete descriptions of conjugated tooth surfaces. Algorithm of determination of the contact point is based on determination of distances between the point on profile of chosen cross-section of male rotor and points of conjugated profiles of female rotor, that create a set of cross-sections, which occurred in vicinity of male rotor's cross-section, Fig. 10. Points of conjugated tooth surfaces of the male rotor 3 and the female rotor 2 which satisfy condition $\left\| \mathbf{r}_{L_{\psi,u}} - \mathbf{r}_{K_{m,n}} \right\| < \delta \wedge \delta \to 0$ are chosen as coalescent points that create the point of contact of both surfaces. The condition $\left\| \mathbf{n}_{L_{\psi,u}} \times \mathbf{n}_{K_{m,n}} \right\| \doteq 0$ creates further condition that is necessary for contact of surfaces at common point. In this term $\mathbf{n}_{A_{i,j}}$ are unit normal vectors of both surfaces at the point of contact L. If both conditions are fulfilled then the pair of points creates the common point of both surfaces that is the point of contact.

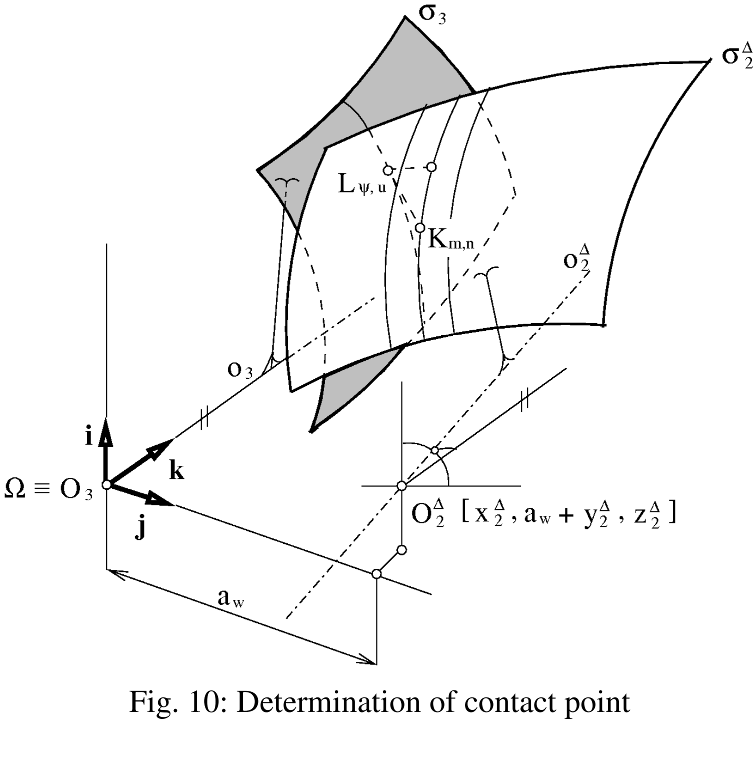

Fig. 10: Determination of contact point

Dependence of vector components of contact point position on rotation of male rotor is shown in Fig. 11. The location of contact point on teeth of male rotor, Fig. 9, in time-interval is shown in Fig. 12, where the time-interval is represented with rotation of male rotor.

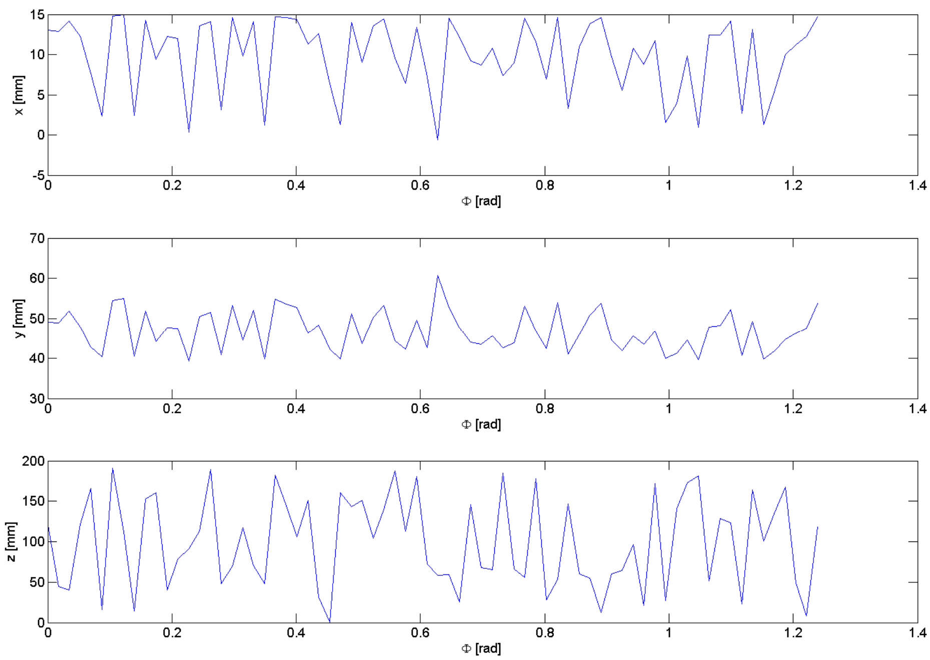

Fig. 11: Contact point position vector components

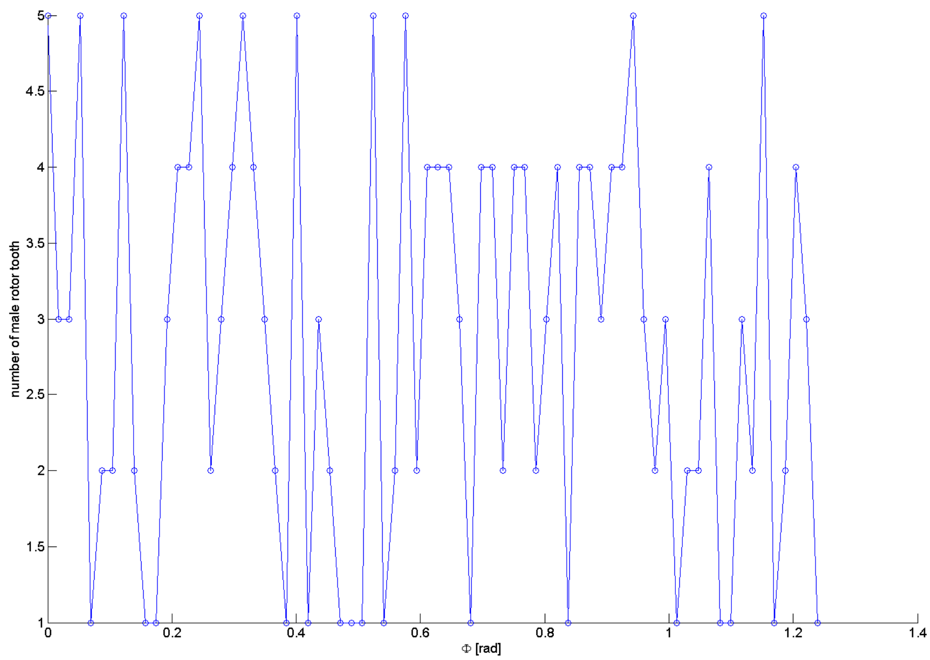

Fig. 12: Location of contact point on teeth of male rotor

5. Conclusion

In this contribution the contact of teeth of screw injected compressors with skew position of axes of rotors, which is caused by seating displacement of both rotors, was solved. The seating deformation, which is caused by force and heat deformation of housing and bearing separately, was considered constant in the selected time level. Contact point transposes on tooth surfaces of both rotors in time period. Transposition of contact the point position, which did not solve till now on this kind of tooth surfaces, could be source of the operational vibration of screw machines.

Acknowledgement

The work has been supported by the research project MSM 4977751303.

References

Fröhlich, J. (1980) *Technika uložení s valivými ložisky* (in Czech). SNTL, Praha.

Kleisner, V. (2006) *Temperature deformation of housing of screw compressor* (in Czech). Bachelor thesis, Plzeň.

Stosic, N., Smith, I.K., Kovacevic, A. (2003) Rotor interface as a criterion for screw compressor design. *Journal of Engineering Design*, Vol. 14, No 2, Taylor & Francis Ltd, pp. 209-220.

Švígler, J., Albl, P. (1995) *Screw compressors II*, Analysis of geometry of screw compressors teeth (in Czech). Research report 102-06-95, ZČU, Plzeň.

Švígler, J., Machulda, V. & Siegl, J. (2006) Deformation of Screw Machine Housing under Force Field and its Consequences. *VDI Berichte Nr.1932 Schraubenmaschinen 2006*, Dortmund, pp. 377-388.